Virology 535 (2019) 1–10

Contents lists available at ScienceDirect

Virology

journal homepage: www.elsevier.com/locate/virology

# Duration of seminal Zika viral RNA shedding in immunocompetent mice inoculated with Asian and African genotype viruses

Erin M. McDonald[a], Nisha K. Duggal[a,1], Mark J. Delorey[a], James Oksanish[a], Jana M. Ritter[b], Aaron C. Brault[a,*]

[a] Division of Vector-borne Diseases, Centers for Disease Control and Prevention, Fort Collins, CO, USA
[b] Division of High-Consequence Pathogens and Pathology, Centers for Disease Control and Prevention, Atlanta, GA, USA

ARTICLE INFO

*Keywords:*
Zika virus
Pathogenesis
Mouse model
Sexual transmission

ABSTRACT

Prior to the emergence of Asian genotype Zika virus (ZIKV) in the Western hemisphere, sexual transmission in humans was documented. Sexual transmission by African genotype ZIKVs has not been assessed in laboratory animal models, due to rapid and high mortality rates of immunodeficient mice following inoculation. To overcome these limitations, immunocompetent C57Bl/6 mice were used to longitudinally assess Asian and African genotype ZIKV sexual transmission potential. Furthermore, to determine if enhanced pathogenesis of African genotype ZIKVs is due to structural determinants, PRVABC59 prM/E was replaced with African MR766 prM/E (chimeric ZIKV). The African genotype and chimeric ZIKV elicited greater pathogenic effects in the male reproductive tract and generated higher viremias. Yet, the duration, magnitude and efficiency of seminal shedding of infectious virus and viral RNA were similar between chimeric-, African and Asian genotype ZIKV-inoculated mice. These data show that increased male reproductive tract pathology does not increase sexual transmission potential.

## 1. Introduction

Sexual transmission as an alternative non-vector borne transmission route for Zika virus (ZIKV) was first posited in 2011, after the spouse of an individual returning from Africa developed a rash and showed serological evidence of ZIKV infection following sexual contact (Foy et al., 2011). Subsequent isolation of ZIKV from seminal fluid of a male experiencing hematospermia was documented during an outbreak in French Polynesia in 2013 (Musso et al., 2015). Consistent with these reports, ZIKV RNA has been detected in multiple bodily fluids of infected individuals, including urine, saliva, vaginal secretions and semen (Mead et al., 2018a; Moreira et al., 2017). Long-term persistence of ZIKV RNA in semen is common, with approximately 50% of infected men shedding ZIKV RNA in semen for 42–54 days following illness onset. Furthermore, approximately 5% of men shed detectable ZIKV RNA as far out as 139–186 days post illness onset (Mead et al., 2018b; Huits et al., 2017; Paz-Bailey et al., 2018; Medina et al., 2019). While semen samples are more frequently viral RNA positive than positive for infectious virus, infectious virus has been detected in semen ranging from fifteen to sixty-nine days post illness onset (Mead et al., 2018b; Medina et al., 2019; Garcia-Bujalance et al., 2017).

Long-term ZIKV RNA shedding in semen also occurs in nonhuman primate (NHP) and murine models. In rhesus macaques, viral RNA was detected in semen 28 days post inoculation (dpi) (Osuna et al., 2016) and in type I/II receptor knockout (AG129) mice, viral RNA persisted for weeks after infectious virus was no longer detected in semen (Duggal et al., 2017a). The cellular reservoir that leads to persistent viral RNA shedding is unknown, but NHP models have confirmed the male reproductive tract (MRT) tropism of Asian lineage ZIKVs (Osuna et al., 2016; Koide et al., 2016). In murine models, both African and Asian genotype ZIKVs replicate in a variety of cell types/tissues in the MRT (Duggal et al., 2017a; Govero et al., 2016; McDonald et al., 2018; Chan et al., 2016). In mice, viral replication in epididymal epithelial cells and infiltrating leukocytes was correlated with sexual transmission potential (McDonald et al., 2018). Consistent with these data, other studies have shown that ZIKV can be sexually transmitted, either by copulation between male and female AG129 mice (Duggal et al., 2017a, 2018), or by a coitus free model of sexual transmission using fluid from epididymides of ZIKV-inoculated *Ifnar1*$^{-/-}$ mice for intravaginal inoculations of naïve female *Ifnar1*$^{-/-}$ mice (Clancy et al., 2018a). Similar assessments for direct sexual transmission potential have not been made with African genotype ZIKV strains, which elicit rapid and high

* Corresponding author. 3156 Rampart Road, Fort Collins, CO 80521, USA.
*E-mail address:* abrault@cdc.gov (A.C. Brault).
[1] Current address: Department of Biomedical Sciences and Pathobiology, Virginia Polytechnic Institute and State University, Blacksburg, VA.

https://doi.org/10.1016/j.virol.2019.06.010
Received 16 May 2019; Received in revised form 11 June 2019; Accepted 13 June 2019
Available online 20 June 2019

mortality rates in immunodeficient mouse models, thus precluding assessment of sexual transmission by inoculated males (McDonald et al., 2017).

This study assessed shedding of ZIKV in semen following inoculation of immunocompetent mice with Asian or African genotype ZIKV isolates. Transient knockdown of type I IFN signaling in C57Bl/6 mice resulted in delayed and/or reduced mortality following inoculation with both African and Asian genotype ZIKV strains compared to similar inoculations of type I/II receptor deficient (AG129) mice. Furthermore, the African and Asian genotype ZIKV strains demonstrated similar sexual transmission potential and duration of ZIKV RNA shedding in semen. These data confirm that sexual transmission of ZIKV is not a recent adaptation, but rather is conserved between African and Asian genotype ZIKV strains. Mice inoculated with a chimeric infectious ZIKV clone, in which PRVABC59 prM/E was replaced with MR766 prM/E, demonstrated greater pathogenic effects in the MRT and higher viremia compared to mice inoculated with Asian genotype ZIKVs.

## 2. Materials and methods

**Virus isolates and recombinant viruses.** The virus isolates used in this study were: PRVABC59 (Puerto Rico 2015; Vero passage 3), P6-740 (Malaysia 1966; suckling mouse passage 6, Vero passage 3), FSS13025 (Cambodia 2010; Vero passage 4), DakAr 41524 (Senegal 1984; AP61 passage 1, C6/36 passage 1, Vero passage 4), and MR766 (Uganda 1947; suckling mouse brain passage 149, Vero passage 2). The MR766 isolate used in these studies does not contain a four amino acid deletion in the E protein common in other passaged isolates (Duggal et al., 2017b). A two plasmid ZIKV PRVABC59 infectious cDNA system was used to engineer all mutations and recombinant viruses (Weger-Lucarelli et al., 2017). The PRVABC59 infectious clone differs from the original PRVABC59 isolate by a non-synonymous mutation at E−330 (E-V330L). The infectious clone (hereafter referred to as E−330L) was mutated using *In Vivo* Assembly cloning (Garcia-Nafria et al., 2016) to make the reverse substitution (E-L330V) and is referred to as E−330V (Duggal et al., 2019). To generate the chimeric prM/E ZIKV ic, the nucleotide sequence of prM/E from MR766 (HQ234498) was synthesized as a gene block, with two synonymous mutations made in the envelope sequence to remove ApaL1 restriction sites (IDT, San Jose, CA). Using the NEBuilder HiFi DNA Assembly Master Mix (New England Biolabs, Ipswich, MA), this gene block was cloned into the first plasmid of the two-part ZIKV infectious clone system by Gibson assembly. The structural protein chimeric virus was generated with the prM/E of MR766 as this African isolate was previously shown to consistently result in mortality in intracranially inoculated immune competent mice from a wide age range and to generate high titers and induce rapid mortality in AG129 mice (McDonald et al., 2017; Duggal et al., 2017b). The assembled product was transformed into chemically competent *E. coli*. Clones were verified by sequencing. The two plasmids were ligated and RNA was transcribed from the full-length infectious clone DNA using the AmpliScribe T7 High Yield Transcription kit (Lucigen). The RNA transcription reaction was transfected into Vero cells using MessengerMax Lipofectamine reagent (ThermoFisher). Supernatant was harvested when cytopathic effect was observed, and virus titrations were carried out by plaque assay on Vero cells.

**Mouse experiments.** 12-week-old male C57BL/6 mice (Charles River, Wilmington, MA) were acclimatized for at least two weeks in the ABSL-2 animal facility at the Division of Vector-Borne Diseases at the Centers for Disease Control and Prevention (Fort Collins, CO). 14- to 18-week old male mice were used for the experimental inoculation studies. One day prior to inoculation (−1 dpi) with virus, the mice were injected intraperitoneally (i.p.) with 2.0 mg of anti-mouse Interferon Alpha/Beta Receptor 1 (MAb-5A3; Leinco Technologies, St. Louis, MO). At dpi 1 and 4, mice were similarly i.p. treated with 0.5 mg of MAb-5A3. This dosing schedule was described previously and is based on the half-life of MAb-5A3 being 5.2 days when used at 2.0 mg (Smith et al., 2017; Lazear et al., 2016; Sheehan et al., 2006).

C57BL/6 mice were inoculated subcutaneously in their rear footpad with a 10 μL inoculum containing $10^3$ PFU of ZIKV strain PRVABC59, P6-740, FSS 13025, MR766, DakAr 41524, or ZIKV infectious clone (ic) E−330L, E−330V, or prM/E chimeric virus. Three mice from each inoculation group (except from the MR766-and DakAr 41524-inoculated groups) were chosen randomly and euthanized on dpi 8 to compare to mice from the MR766-and DakAr 41524 inoculated groups (which met clinical criteria for euthanasia on dpi 7–12). For the remaining mice in each group, mice were euthanized when clinical evidence of disease was observed or when dpi 28–33 was reached (terminal end point). Mice were euthanized by cervical dislocation while under isoflurane-induced deep anesthesia. Tissues and serum were collected at the time of euthanasia.

Semen from male C57BL/6 mice were collected as previously described (Duggal et al., 2017a; McDonald et al., 2017). Inoculated male mice were housed individually, and each evening (beginning on dpi 6) three female CD-1 mice were introduced into the cage. The following morning, females were examined for evidence of a copulatory plug. Mated females with a copulatory plug were euthanized and then processed immediately to collect semen by flushing both horns of the uterus with 500 μL of BA-1 media. Semen was stored at −80 °C until titrated for infectious titers or RNA was extracted for qRT-PCR.

**Viral Quantification.** Brain, testis and seminal vesicle tissues were weighed and then homogenized using a pestle in an equal volume of BA-1 medium, and then clarified by centrifugation. Eyes were either resuspended in 25 μL of BA-1 medium or weighed and resuspended in an equal volume of BA-1 medium, and then homogenized using a pestle, followed by clarification by centrifugation. The epididymides were minced with a scalpel in 500 μL of BA-1 media. Clarified tissue homogenates and epididymal cell suspensions and semen collections were serially diluted for titration by plaque assay. For tissues and serum from mice inoculated with the ZIKV isolates, E−330L, or prM/E chimeric virus, the secondary overlay containing neutral red for the Vero cell plaque assay was added four days post-inoculation. For tissues and serum from mice inoculated with E−330V, the secondary overlay was added five days post-inoculation due to the small plaque morphology of this virus. The limit of detection for tissues (brain, testis, and seminal vesicle) was 1.7 $\log_{10}$ PFU/gram, the limit of detection for eye titers was 2.0 $\log_{10}$ PFU/eye, for serum titer was 2.0 $\log_{10}$ PFU/mL and for semen was 0.4 $\log_{10}$ PFU/ejaculate.

**ZIKV RNA Quantification.** Semen was denatured in 10 mM DTT, and RNA extracted from the denatured samples using the MagMAX Viral RNA Isolation Kit (Ambion). ZIKV RNA was quantified using real-time RT-PCR primers and probe as described previously (Lanciotti et al., 2007). A standard curve was generated by *in vitro* transcription (AmpliScribe T7 High Yield transcription kit) of a plasmid containing a fragment of ZIKV spanning genomic position nucleotides 859–1278. The detection limit for this assay was 2.0 $\log_{10}$ RNA copies per ejaculate (Lanciotti et al., 2007).

**Time to clearance (of ZIKV RNA in semen) model development.** The data used for model assessment were from C57BL/6 immunocompetent mice pretreated with monoclonal antibody against IFNAR1 and inoculated with PRVABC59 (n = 5), FSS13025 (n = 5), P6-740 (n = 5), MR766 (n = 5), DakAr 41524 (n = 5) or ZIKV ic prM/E chimeric virus (n = 6).

A male mouse was considered to have cleared ZIKV RNA in their semen once it had two negative samples in a row, followed by no further positive samples, or if it was negative on the last day of the study. For mice that were negative by the end of the study, clearance of ZIKV RNA was assumed to have occurred between the day of the last positive sample and the day of the next negative sample (interval censoring). For mice that were still positive at their last collection, time to clearance was right censored at the day of the last positive sample. A two-parameter Weibull distribution was fit to the time to clearance, allowing both the scale and the shape parameters to vary by strain.

Standard diagnostics were performed to ensure model fit.

**Histopathology and RNA *In Situ* Hybridization.** After mice were euthanized, tissues were immediately placed into 10% neutral buffered formalin for 3 days and then transferred to and stored in a 70% ethanol solution prior to processing. Sections were cut at 4 μm and stained by routine hematoxylin-eosin or by *in situ* hybridization (ISH). Probe sets targeting the positive-strand ZIKV RNA genome were used with the ViewRNA ISH tissue assay (ThermoFisher). As a negative control, tissue sections from a PBS mock-inoculated C57BL/6 uninfected male mouse were stained using the ZIKV (+) probe set. As a positive control, tissues were stained using probes against the housekeeping murine mRNAs GAPDH, PIPB, and β-actin. Tissue sections were de-paraffinized and underwent an optimized View RNA ISH tissue assay, with pre-treatment and protease treatments lasting 7 min each. Positive staining (red punctate staining) was detected using an alkaline-phosphatase label probe. Nuclei were counterstained with Gill's Hematoxylin I.

## 3. Results

**African genotype ZIKV isolates are more pathogenic than Asian genotype ZIKV isolates in immunocompetent mice.** Since the sexual transmission potential of African genotype ZIKV strains could not be studied in immunodeficient mouse models due to rapid and high mortality rates following inoculation (McDonald et al., 2017), an immunocompetent mouse model was used to assess pathogenesis and sexual transmission potential of multiple Asian and African genotype ZIKVs. Previous studies demonstrated that C57Bl/6 mice treated with anti-Ifnar1 monoclonal antibody MAb-5A3 and inoculated with African or Asian genotype ZIKVs develop viremia with subsequent infection of peripheral organs, including the murine MRT (Govero et al., 2016; Smith et al., 2017). Therefore, immunocompetent C57BL/6 male mice were treated with MAb-5A3 and inoculated in groups of 8–9 with $10^3$ PFU of Asian genotype ZIKV strains (PRVABC59, FSS 13025 or P6-740), African genotype ZIKV strains (DakAr 41524 or MR766), or infectious clone derived viruses (E−330L, E−330V or prM/E chimeric virus).

Only mice inoculated with African genotype ZIKV strains (MR766 or DakAr 41524) exhibited mortality (Fig. 1A). Mice inoculated with MR766 had a median survival time of 9.8 days, and 75% succumbed to infection. For mice inoculated with DakAr 41524, 43% of the mice were euthanized after displaying clinical signs of disease (mice were euthanized on dpi 11 and 12). Mice inoculated with MR766 and DakAr 41524 lost significantly more weight than mice inoculated with Asian genotype ZIKVs (Fig. 1B–F). Significant weight loss was first observed on dpi 7 for mice inoculated with MR766 and on dpi 8 for mice inoculated with DakAr 41524 ($p \leq 0.0001$ MR766 and DakAr 41524 vs PRVABC59, FSS 13025; $p \leq 0.0001$ DakAr 41524 vs P6-740; $p < 0.01$ MR766 vs P6-740). Mice inoculated with Asian genotype ZIKV strains only lost between 3 and 5% of their initial body weight and this weight loss occurred early following inoculation (Fig. 1D–F).

Since the African genotype ZIKVs elicited mortality in immunocompetent mice, we assessed whether the prM/E structural genes from African ZIKVs could confer enhanced pathogenic effects in an Asian genotype ZIKV. Using a reverse genetics system based on PRVABC59, a recombinant chimeric virus was generated in which prM/E was replaced with prM/E from African MR766 ZIKV (prM/E chimeric virus). prM/E from MR766 was chosen as previous studies have reported similar neurovirulence of MR766 and DakAr 41524 following intracranial inoculation of immunocompetent CD-1 mice (Duggal et al., 2017b). Furthermore, there are only four amino acid differences between the prM/E sequence of MR766 and DakAr 41524 (E-Y158H, E-K283R, E-I341R, E-V343A). This recombinant prM/E chimeric virus was directly compared to a parental infectious clone derived virus containing either a non-synonymous variant at E−330 (E-V330L), recently shown to result in attenuated pathogenesis in immunodeficient mice, or the clone representative of the original PRVABC59 isolate (E−330V) (Duggal et al., 2019).

100% of the mice inoculated with prM/E chimeric virus, E−330L, and E−330V survived to the experimental endpoint (Fig. 1A). Thus, the African prM/E structural genes did not increase mortality of the Asian genotype virus. Furthermore, mice inoculated with chimeric virus or the parental infectious clone viruses lost significantly less weight than mice inoculated with the African ZIKVs (Fig. 1B–C, 1G-I; dpi 7–11; $p \leq 0.0001$). We did not find evidence of differential weight loss between mice inoculated with the Asian genotype ZIKVs versus mice inoculated with the chimeric virus or the infectious clone derived ZIKVs.

**African genotype ZIKV isolates replicate to higher titers in blood, brain, and eye.** Viremia was transient for all groups of mice, with infectious virus being detected on dpi 3 through 7 (Fig. 2A–C). The highest viremia titers were observed in the mice inoculated with MR766 and DakAr 41524 (Fig. 2A), with significant differences in titer magnitude observed between MR766 and DakAr41524 at dpi 5 and between both of the African ZIKVs vs all other groups at dpi 5 ($p < 0.0001$; $p < 0.01$ for MR766 vs P6-740). For mice inoculated with PRVABC59 or FSS13025, peak viremia occurred on dpi 3 (Fig. 2B). In mice inoculated with P6-740 or with E−330V/L, peak viremia was delayed until dpi 5 (Fig. 2B–C). Mice inoculated with the chimeric virus exhibited significantly higher serum titers than ZIKV ic E−330V and E−330L on dpi 3 and 5, and higher serum titers than PRVABC59 and FSS 13025 on dpi 5 (Fig. 2B–C). However, the prM/E chimeric virus titers were significantly lower than those of mice inoculated with African genotype ZIKVs (Fig. 2A–C).

As early as dpi 7, infectious virus was present in the eyes and brains of C57Bl/6 mice inoculated with African genotype ZIKV strains (Fig. 3A–B). The mean eye titer for DakAr-inoculated mice was significantly higher than the mean titer of MR766-inoculated mice (6.8 $\log_{10}$ PFU/eye vs 3.5 $\log_{10}$ PFU/eye; $p < 0.0001$). Only one FSS13025-inoculated mouse had infectious virus in their eye at dpi 8. Infectious virus was absent from the eyes of prM/E chimeric-, E−330V- or E−330L-inoculated mice on dpi 8 (data not shown).

All mice in the DakAr 41524- and MR766-inoculation groups had infectious virus present in the brains from dpi 7 to 12 (4.2 and 5.2 $\log_{10}$ PFU/gram, respectively; Fig. 3B). In contrast, less than half (4 of 9) of the mice inoculated with Asian genotype ZIKV isolates had infectious virus in the brain on dpi 8. The mean titers were 1.8 (PRVABC59), 2.0 (FSS 13025) and 3.2 (P6-740) $\log_{10}$ PFU/gram of brain tissue. Although there was no significant difference in brain titers between the two African genotype ZIKV strains ($p = 0.6998$), MR766-inoculated mice had significantly higher brain titers than PRVABC59-, FSS 13025-, prM/E chimeric virus-, E−330V- and E−330L-inoculated mice ($p < 0.05$).

**The epididymides are crucial for sexual transmission potential.** Viral dissemination to the MRT was also assessed. On dpi 8, infectious virus was absent from the seminal vesicle and testis in mice inoculated with Asian genotype ZIKV isolates, with the exception of one P6-740-inoculated mouse. Only a subset of prM/E chimeric- and E−330V-inoculated mice had infectious virus in these tissues, with no significant differences found. In contrast, the testes and seminal vesicles of mice inoculated with MR766 and DakAr 41524 were robustly infected and had significantly higher titers (7.3 and 7.9 $\log_{10}$ PFU/gram of testis and 3.3 and 2.5 $\log_{10}$ PFU/gram of seminal vesicle, respectively) than the other groups (Fig. 4A–B).

Infectious virus was present in the epididymides from all group of inoculated mice (with the exception of E−330L), even when infectious virus was absent from the the testes and seminal vesicles (Fig. 4C). The epididymal titers from mice inoculated with MR766 (6.4 $\log_{10}$ PFU/epididymides), DakAr 41524 (6.4 $\log_{10}$ PFU/epididymides) and the prM/E chimeric virus (6.8 $\log_{10}$ PFU/epididymides) were significantly higher than epididymal titers from mice inoculated with PRVABC59 or E−330L (1.9 and 0.7 $\log_{10}$ PFU/epididymides, respectively). There were no significant differences found in epididymal titers between prM/E chimeric-inoculated mice vs mice inoculated with African genotype

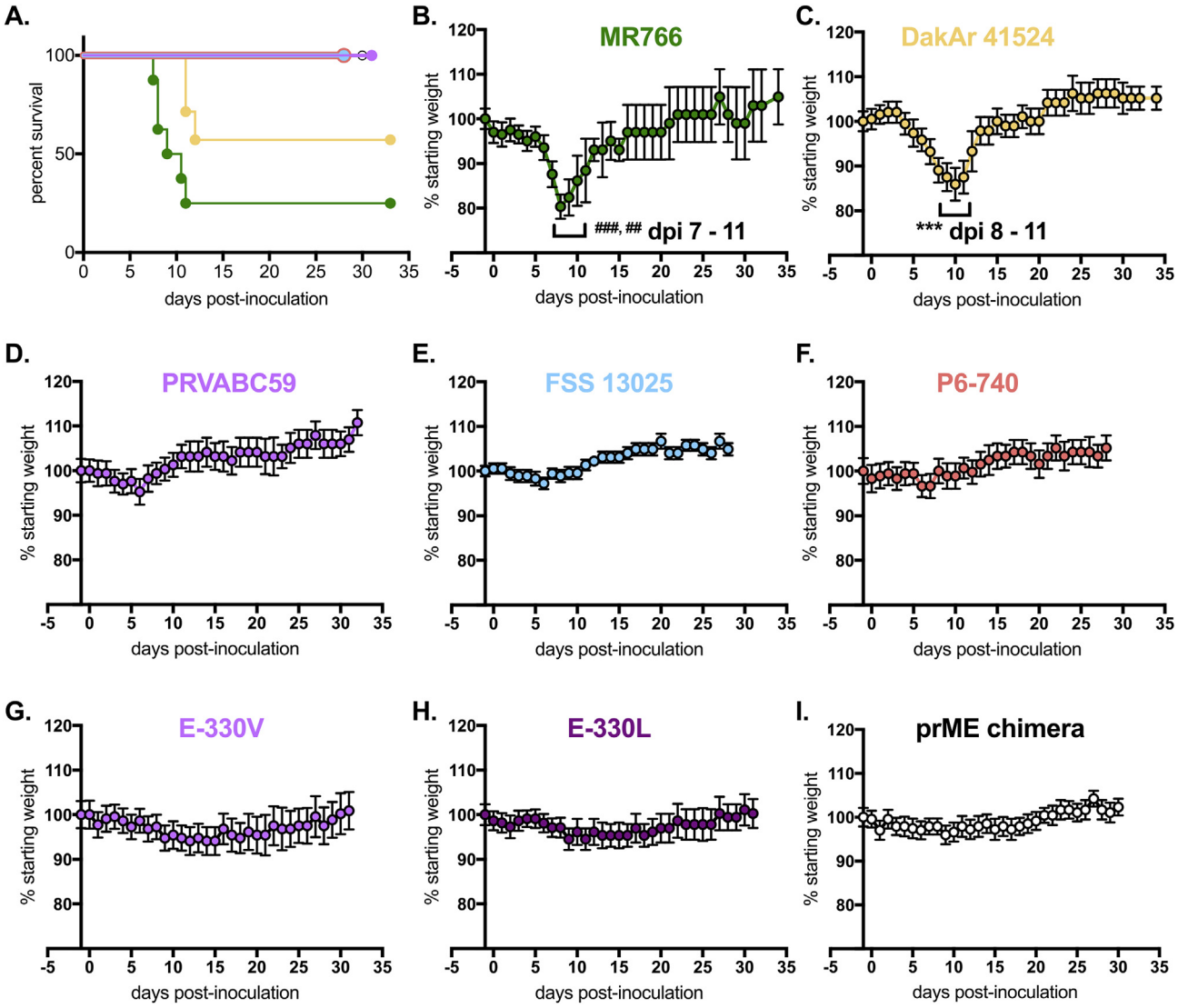


**Fig. 1. African genotype ZIKV isolates are more pathogenic in immunocompetent mice.** C57BL/6 immunocompetent mice were treated with monoclonal antibody against IFNAR1 one day prior to inoculation with either DakAr 41524 (n = 8), MR766 (n = 8), PRVABC59 (n = 8), FSS13025 (n = 8), P6-740 (n = 8), E330V ZIKV ic (n = 8), E330L ZIKV ic (n = 8), or ZIKV ic prM/E chimeric virus (n = 9). (**A**) Percent survival of mice post-inoculation. (**B–I**) Average weight of mice post-inoculation, represented as a percentage of initial weight. Error bars represent standard deviations. p-values determined by two-way ANOVA (Tukey's multiple comparisons test).
***p ≤ 0.0001 DakAr 41524 vs PRVABC59, FSS 13025, P6-740, E−330V, E−330L, prM/E chimeric virus.
###p ≤ 0.0001 MR766 vs PRVABC59, FSS 13025, E−330V, E−330L, prM/E chimeric virus.
##p < 0.01 MR766 vs P6-740.

ZIKVs (p = 0.9).

To assess sexual transmission potential of the different ZIKV strains, ejaculates were collected from inoculated male mice indirectly by flushing the uteri of mated females. Infectious virus in semen was detected as early as dpi 6 for both the African genotype ZIKV isolates (Fig. 5A–B). For FSS 13025- and P6-740-inoculated mice, ejaculates contained infectious virus beginning on dpi 8–12 (Fig. 5D–E). Peak titers in semen for either African or Asian genotype ZIKV inoculated mice occurred from dpi 9–12 and were similar in titer, ranging from 2.3 to 4.0 $\log_{10}$ PFU/ejaculate (Table 1; no significant differences found). No infectious virus was detected in the ejaculates from mice inoculated with the PRVABC59 isolate, but infectious virus was detected in ejaculates from mice inoculated with E−330L and E−330V. Despite the lack of infectious virus in the epididymides on dpi 8 from a subset of the E−330L-inoculated mice, there was infectious virus present in semen from the other mice in this group, beginning on dpi 9 (Fig. 5H; Table 1). The time period that infectious virus was found in semen did not differ among the three groups of mice inoculated with the infectious clone-derived viruses, which ranged from approximately dpi 9 to dpi 19 (Fig. 5A–H; Table 1).

Persistent viral RNA shedding in semen has been repeatedly observed following ZIKV infection in humans. Therefore, viral RNA in ejaculates was quantified by qRT-PCR. Consistent with previous reports, viral RNA was more frequently detected in semen than was infectious virus: only 12–28% of ejaculates had detectable infectious virus versus 40–71% that were positive for ZIKV RNA (Fig. 5I-P; Table 1). Viral RNA was detected in some ejaculates at the experimental end point (dpi 28–33; Fig. 5I-P), demonstrating this immunocompetent mouse model could be useful to study long-term viral RNA shedding in semen.

Since viral RNA was consistently detected in semen as far out as dpi 26–30 (which represented the last ejaculates collected before the experimental endpoint), the brain, eye and MRT tissues from the terminal end point were screened by plaque assay (Supplemental Fig. 1). At the

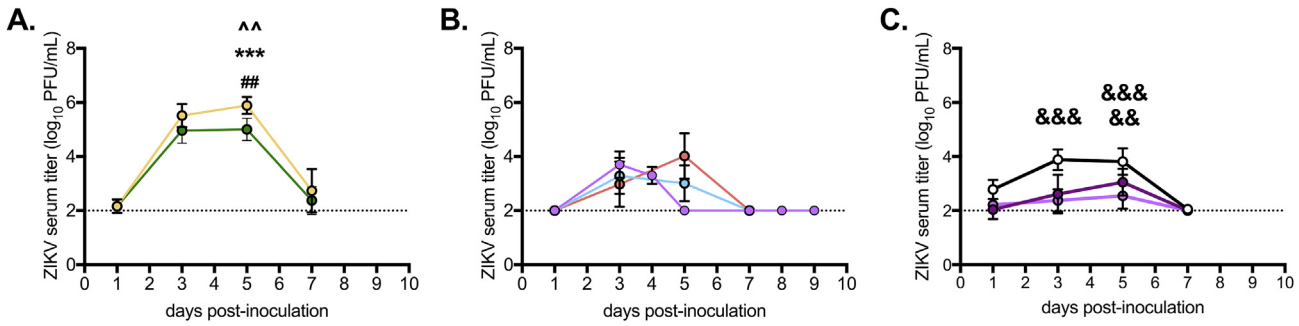


**Fig. 2. Viremia of immunocompetent mice inoculated with ZIKV isolates and ZIKV infectious clone derived viruses.** Viremia of mice on days 1,3, 5 and 7 post-inoculation with (**A**) African genotype ZIKV isolates (n = 7–8 mice per timepoint per group), (**B**) Asian genotype ZIKV isolates (n = 4–8 mice per time point for PRVABC59; n = 8 mice per time point for other Asian genotype ZIKV isolates), and (**C**) infectious clone derived viruses (n = 9 mice per time point per group). p-values determined by two-way ANOVA (Tukey's multiple comparisons test).
^^ $p < 0.01$ MR766 vs DakAr 41524.
***$p < 0.0001$ MR766 and DakAr 41524 vs PRVABC59, FSS 13025, E−330V, E−330L, prM/E chimeric virus, and DakAr 41524 vs P6-740.
##$p < 0.01$ MR766 vs P6-740.
&& $p < 0.01$ prM/E chimeric virus vs E−330L.
&&& $p < 0.0001$ prM/E chimeric virus vs E−330V.

terminal time points, no infectious virus was detected in the eye or brain. In the MRT, no infectious virus was detected in the seminal vesicles. However, in the testis, two mice (one PRVABC59- and one P6-740-inoculated mouse) had infectious virus: 5.3 and 4.5 $\log_{10}$ PFU/gram, respectively. In the epididymides, the same PRVABC59-inoculated mouse had infectious virus (4.0 $\log_{10}$ PFU/epididymides). An MR766-inoculated mouse also had detectable infectious virus in the epididymides at the terminal time point (3.2. $\log_{10}$ PFU/epididymides). When the tissues from mice inoculated with the infectious clone derived viruses were screened, two mice inoculated with E−330V virus had virus in the testis and epididymis, with an average titer of 3.2 $\log_{10}$ PFU/gram in the testis and 1.5 $\log_{10}$ PFU/epididymides. Based on these results, the epididymis and/or testis could be a reservoir from which ZIKV RNA is shed long-term in semen.

**African genotype and prM/E chimeric ZIKV cause epididymal pathology**. Histopathologic evaluation and in situ hybridization for ZIKV RNA was performed on male reproductive tract tissues collected at dpi 8 from mice inoculated with MR766 (n = 2), ZIKV ic E−330V (n = 2), ZIKV ic E−330L (n = 3) or the prM/E chimeric virus (n = 3) to assess pathology and viral RNA distribution. Of the tissues examined (testis, epididymis, vas deferens, and seminal vesicle), the epididymis had the most pronounced histopathologic alterations and was the only tissue to consistently show viral RNA detection by ISH for all 4 ZIKV strains evaluated. Epididymis tissue from MR766-inoculated animals had patchy tubular epithelial degeneration and variable tubular dilation with tubulointerstitial inflammation. These changes were most severe, and sometimes accompanied by tubular rupture, within the proximal segments of the epididymal head and body (Fig. 6, top left); the tail was much less affected.

Epididymides from prM/E chimera-inoculated animals had similar tubular epithelial degeneration and dilation, with more prominent interstitial, predominantly mononuclear inflammation, but without tubular rupture as seen in MR766 (Fig. 6, top middle-left). Changes were again most prominent in the epididymal head and body, with sparing of the tail. Epididymides from E−330V and E−330L inoculated animals lacked epithelial necrosis, and had no to minimal interstitial inflammation in epididymal heads (Fig. 6, top right and middle-right). One E−330V epididymis had scattered sperm granulomas, which were interpreted as incidental. For MR766-and prM/E chimera-inoculated mice, ZIKV RNA labeling by ISH was seen in epididymal tubular epithelium and intraluminal sloughed cells, and generally correlated in amount and localization with necrosis and inflammation. For E−330V and E−330L animals, rare, scattered epithelial staining was seen in the proximal epididymal segments (Fig. 6, middle row).

Testis tissue from MR766-inoculated mice showed rare, scattered, sloughed seminiferous epithelial cells and moderate staining by ZIKV ISH (Fig. 6, bottom left). Testis tissue from prM/E chimera showed very rare seminiferous epithelial sloughing, and were negative for ZIKV RNA by ISH (Fig. 6, bottom middle-left). Testis tissue from E−300V and E−330L inoculated mice had no histopathologic abnormalities or staining by ZIKV ISH (Fig. 6, bottom right and middle-right). Sections of vas deferens and seminal vesicle tissue from all animals in all groups had no histopathologic abnormalities and no staining by ZIKV ISH.

**Sexual transmission modeling of mice inoculated with Asian and African genotype ZIKVs and prM/E chimeric ZIKV.** To determine if there were differences in the mean duration (dpi) of viral RNA shedding in semen in mice inoculated with African or Asian genotype ZIKVs, a Weibull distribution was fitted to the data. Male mice that successfully mated were grouped as follows: African genotype ZIKV group (2 mice inoculated with MR766 and 7 mice inoculated with

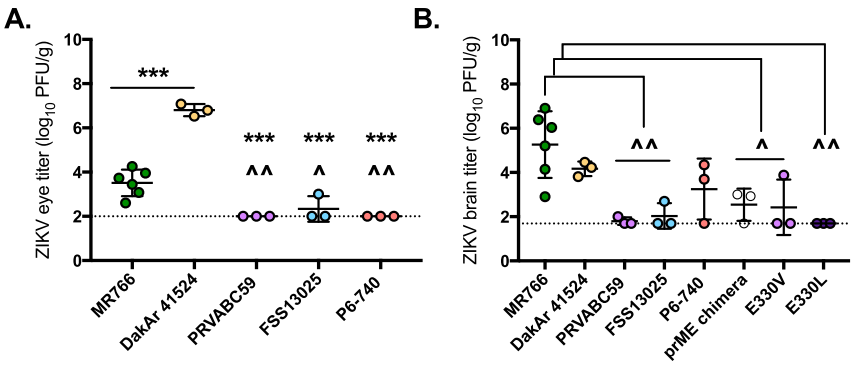


**Fig. 3. Only African genotype ZIKV isolates infect the eye during acute infection.** ZIKV titer in eye and brain collected on day 8 post-inoculation for PRVABC59-, FSS13025- and P6-740-, and chimera-inoculated mice (n = 3 each) and on days 7–12 post-inoculation for MR766- (n = 6) and DakAr 41524- (n = 3) inoculated mice. p-values determined by One-way ANOVA (Tukey's multiple comparisons test).
^ $p < 0.05$; ^^ $p < 0.01$ MR766 vs PRVABC59, FSS 13025, P6-740.
***$p < 0.0001$ DakAr 41525 vs MR766, PRVABC59, FSS 13025, P6-740.

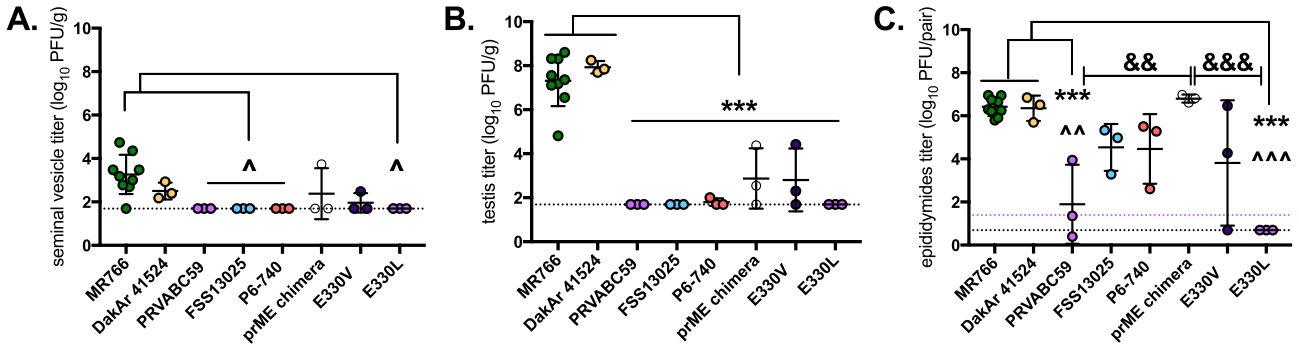


**Fig. 4. All ZIKV isolates infect the epididymis during acute infection.** ZIKV titer in seminal vesicles (**A**), testes (**B**), and epididymides (**C**) collected on day 8 post-inoculation for PRVABC59-, FSS13025- and P6-740-inoculated mice (n = 3 each) and on days 7–12 post-inoculation for MR766- (n = 6) and DakAr 41524- (n = 3) inoculated mice. p-values determined by One-way ANOVA (Tukey's multiple comparisons test).
^ $p < 0.05$; ^^^ $p \leq 0.0001$ MR766 vs Asian ZIKV isolates and infectious clone derived viruses.
***$p < 0.0001$ MR766 and DakAr 41524 vs Asian ZIKV isolates and infectious clone derived viruses.
&& $p < 0.01$; &&& $p \leq 0.0001$ prM/E chimera vs PRVABC59, E−330L.

DakAr), Asian genotype ZIKV group (21 mice total; 7 mice per group inoculated with either FSS 13025, P6-740 or PRVABC59) and prM/E chimeric virus group (5 inoculated mice). On average, male mice inoculated with African genotype ZIKVs mated 5.9 times; male mice inoculated with Asian genotype ZIKVs mated 5.1 times; and male mice inoculated with the prM/E chimeric virus mated 7.8 times. Fig. 7 shows

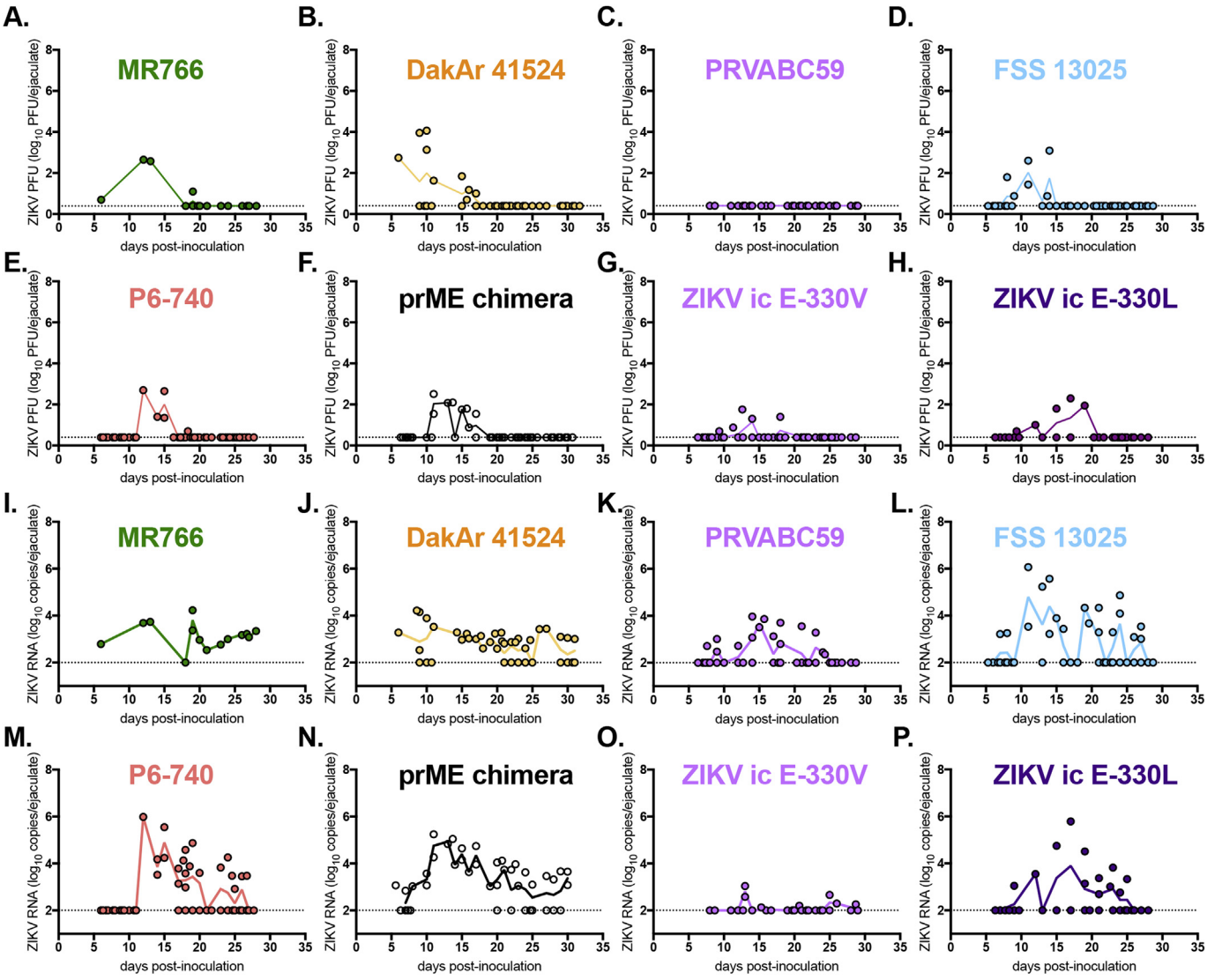


**Fig. 5. Sexual transmission potential of ZIKV isolates in immunocompetent C57BL/6 mice treated with monoclonal antibody against IFNAR1.** Viral titers (**A-H**) and viral RNA copy number (**I–P**) in seminal fluids collected from mice inoculated with ZIKV isolates. Dashed line is limit of detection.

**Table 1**
Infectious virus is shed in semen during a similar time interval for mice inoculated with either African or Asian ZIKV strains.

| Virus Strain | # ejaculate s collected (dpi) | % ejaculates positive for RNA (n) | % ejaculates positive for infectious virus (n) | Infectious range (dpi) | Peak titer log10(PFU/ejac) (dpi) |
|---|---|---|---|---|---|
| MR766 | 14 (6–28) | 93% (13) | 28% (4) | 6–16 | 2.7 (12) |
| Dak Ar41524 | 41 (6–28) | 71% (29) | 24% (10) | 6–18 | 4.0 (9) |
| PRVABC59 | 29 (6–29) | 28% (8) | 0% (0) | N/A | N/A |
| FSS 13025 | 42 (6–28) | 45% (19) | 23% (10) | 8–14 | 3.1 (14) |
| P6-740 | 47 (6–27) | 40% (19) | 12% (6) | 12–15 | 2.7 (12) |
| prM/E Chimera | 42 (7–30) | 71% (30) | 19% (8) | 11–17 | 2.5 (11) |
| E − 330V | 40 (7–28) | 38% (15) | 20% (8) | 9–18 | 1.8 (14) |
| E − 330L | 32 (7–28) | 38% (12) | 15.6% (5) | 9–19 | 2.3 (17) |

the fitted time-to-clearance curves in the upper half of the graph. The lower part of the graph marks the time intervals, in dpi, over which each mouse was estimated to have cleared ZIKV. The p-value of the likelihood ratio test comparing the fitted model to the null model is 0.41, and pair-wise comparisons of the estimated scale and shape parameters of each curve show no statistical differences (Supplemental Fig. 2 shows the 95% confidence regions for each curve, color coded to the curve). Thus, the data provide no evidence whether duration of viral RNA shed in semen differs between mice inoculated with African genotype vs Asian genotype vs prM/E chimeric ZIKVs.

## 4. Discussion

In this study, we show that both Asian and African genotype ZIKVs have similar sexual transmission potential in an immunocompetent mouse model. Here, we demonstrated infection of the epididymides is critical for establishing sexual transmission potential, as infectious virus and viral RNA was detected in the epididymis and in semen days before infectious virus was detected in the seminal vesicle or testis. Viral RNA was shed in semen for the duration of the study, which lasted approximately one month. Persistent viral RNA in semen is a feature described in many human male case reports and has been observed in many large human cohort studies (Mead et al., 2018b; Paz-Bailey et al., 2018). Furthermore, in support of previous studies, infectious virus is present for a short period of time in semen (approximately from day 6–19) following inoculation, but beyond three weeks, only viral RNA is detected (Duggal et al., 2017a).

In this immunocompetent mouse model, African genotype ZIKV strains were more pathogenic than Asian genotype ZIKV strains, as evidenced by greater weight loss, more epididymal pathology and viral RNA staining, and higher viral titers in the serum, testis, seminal vesicle, eye (MR766 and DakAr) and brain (MR766). Despite greater pathology and ZIKV RNA staining by ISH, especially in the MRT, following inoculation of African genotype ZIKVs vs Asian genotype ZIKVs, sexual transmission was not enhanced. To delineate viral genetic determinants of increased pathogenesis of African ZIKVs, we generated a recombinant virus in which prM/E from PRVABC59 was replaced with prM/E from MR766. Although this recombinant prM/E chimeric virus elicited greater tissue damage and viral RNA staining in the epididymis than the parental PRVABC59 clone virus (E − 330V), sexual transmission potential was not increased. Furthermore, mice inoculated with the recombinant prM/E chimeric virus had significantly increased viremias compared to mice inoculated with the PRVABC59 isolate or the E − 330V/E − 330L infectious clone-derived viruses, and thus, the structural genes prM/E are determinants of viremia, but not sexual transmission.

In AG129 mice, the E − 330L mutation was attenuating, as evidenced by decreased neuroinvasiveness, decreased serum viremia and increased median survival times (Duggal et al., 2019). The relative effect of sexual transmission potential of E-330V could not be assessed in AG129 mice due to the extremely high and rapid mortality rate following inoculation with E − 330V. In this current work, we demonstrate decreased pathogenicity of E − 330L and E − 330V vs the African genotype ZIKV MR766 isolate in the murine MRT of immunocompetent

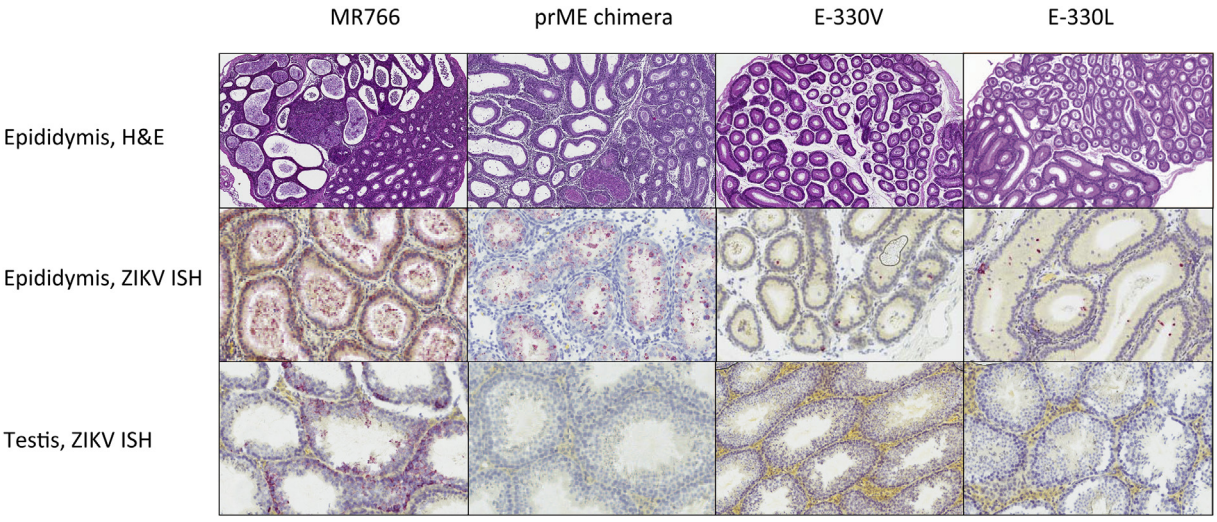


**Fig. 6. Epididymal pathology and epididymal and testicular viral RNA localization by ISH at dpi 8**. Top row: Epididymal heads from MR766 and prM/E inoculated animals showing tubular degeneration and dilation with interstitial inflammation. Epididymidal heads from E − 330V and E − 330L animals are unaffected. Middle row: Epididymis from MR766 showing extensive ZIKV RNA labeling (red staining) within epithelium and luminal cells by in situ hybridization. prM/E chimera epididymis shows less staining than MR766, but more than the rare, scattered epithelial staining seen in E − 330V and E − 330L. Bottom row: Testis from MR766 inoculated animal showing ZIKV RNA labeling (red staining) within seminiferous epithelium by in situ hybridization. Testes from prM/E chimera, E − 330V, and E − 330L inoculated animals have no staining in the testis by ISH.

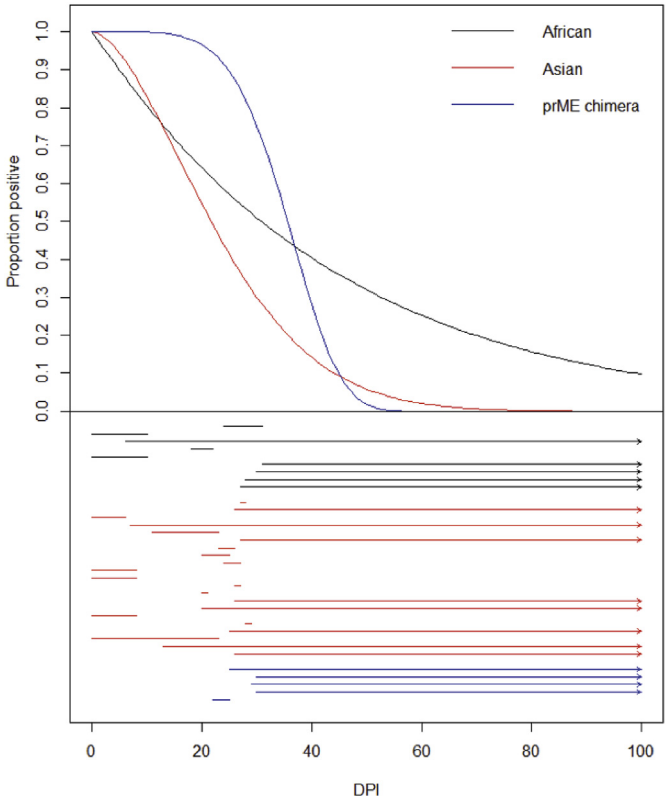


**Fig. 7. Estimated proportion of mice shedding ZIKV RNA in semen.** The top portion of the graph shows the estimated proportion of mice that are still shedding ZIKV RNA in their semen by days post infection. The horizontal segments in the lower part of the graph indicate time periods (days post infection) over which we know a mouse to have gone from shedding to not shedding. Each segment represents a different mouse.

mice. Despite decreased tissue pathogenicity, as demonstrated by pathology and viral titers in the MRT, including a delay in production of infectious virus in the epididymides, mice inoculated with E−330V/L still had the capacity to sexually transmit ZIKV as early as dpi 9.

Infectious virus was cleared from semen by three weeks post-inoculation, similar to previous reports of seminal shedding in type I/II IFN receptor deficient mice (Duggal et al., 2017a; McDonald et al., 2017, 2018). These data indicate that type I interferons and type II interferon (IFN-γ) are not critical for immune-mediated clearance of infectious virus from semen. Thus, alternative anti-viral mechanisms in the murine epididymis must be involved, such as toll-like receptor (TLR) and RIG-1-like receptor (RLR) signaling pathways (Zhu et al., 1950; Palladino et al., 2007). Signaling through these receptors at mucosal surfaces, such as in the female and male reproductive tract, induces production of pro-inflammatory cytokines, including expression of the epithelial-specific type three interferons: IFN-λ1, IFN-λ2 and IFN-λ3 (Zhu et al., 1950; Sommereyns et al., 2008; Zanoni et al., 2017). Epithelial cells, especially those at mucosal surfaces, express IFN-λ receptor (IFNLR), allowing IFN-λ to act in a directed and localized manner (reviewed in (Zanoni et al., 2017)). This is in contrast to type I and type II IFNs, which act systemically due to the universal expression of their respective receptors on nucleated cells.

Type III IFNs have an antiviral role in protecting mucosal surfaces. Much of the work studying the effect of IFN-λ on restricting ZIKV has been modeled in the female reproductive tract (FRT) and in primary cell culture models of the FRT. Primary human trophoblasts produce IFN-λ1 and do not support replication of ZIKV (Bayer et al., 2016). IFN-λ1 and IFN-λ2 are released from 3D cell-line models of human syncytiotrophoblasts and primary synctiotrophoblasts from second trimester placentas (Corry et al., 2017). Tissues from midgestation human pregnancies, and primary human amniotic, vaginal and cervical epithelial cells exhibited reduced ZIKV titers when exogenously treated with IFN-λ (Jagger et al., 2017; Caine et al., 2019; Chen et al., 2017). Treatment of *Ifnar1*$^{-/-}$ dams with exogenous IFN-λ2 decreased the viral titer in both maternal and fetal tissues (Chen et al., 2017). In support of a protective role for IFN-λ, *Ifnlr*$^{-/-}$ mice (treated with an IFNAR1 blocking antibody to establish ZIKV infection) had increased viral titers in the placenta and fetus (Jagger et al., 2017), although the protective effect of IFN-λ in the FRT was dependent upon the mice being in progesterone high diestrous phase (Caine et al., 2019). A protective role for IFN-λ in attenuating ZIKV pathogenesis in the MRT has not been assessed.

Sexual transmission has not been described for other flaviviruses. Dengue virus is capable of infecting the murine MRT of transiently immunodeficient mice only when inoculated directly into the testes. Viral antigen was detected only in the first week following intra-testicular injection, and the virus did not spread to the rest of the reproductive tract (Ma et al., 2016). Spondweni virus (SPONV), the most closely related flavivirus to ZIKV, infects the MRT of AG129 mice, but SPONV RNA was detected in less than 40% of ejaculates and only rarely was infectious virus detected in semen (McDonald et al., 2017). In 2018, a single case report of Yellow Fever virus RNA detected in a semen sample from a convalescent patient was published. Infectious virus was not isolated from the sample, but a complete virus genome was recovered (Barbosa et al., 2018). Wesselsbron virus causes abortions and mortality in pregnant sheep, but whether sexual transmission and subsequent *in utero* transmission is feasible is unknown (Diagne et al., 2017). Thus far, ZIKV is unique amongst flaviviruses in its ability to be sexually transmitted.

Whether long-term persistent infection and subsequent ZIKV RNA shedding has any effects on the health of the MRT has not been resolved. Murine testicular atrophy during acute infection has been observed following ZIKV inoculation. In murine models, persistent infection and immune activation in the tissues of the MRT result in orchitis and/or epididymitis (Clancy et al., 2018b). This has implications for human pathogenesis, as ZIKV infection could negatively impact spermatogenesis. In a recent study, total sperm counts and total motile sperm counts were shown to decrease 60 days after symptom onset in a small cohort of men with laboratory confirmed ZIKV infection. Sperm counts and motile sperm counts recovered in the men as early as 90 days post symptom onset (Joguet et al., 2017). Lastly, although it is established that ZIKV has tropism for the MRT, the potential for recrudescence of productive virus replication following local or systemic immune suppression is currently unknown. This immunocompetent mouse model should serve as a valuable tool to study the long-term effects of viral infection on the MRT, to discern the mechanism of action for clearance of infectious virus from semen and to identify the reservoir(s) for persistent viral RNA shedding in semen.

## Acknowledgements

This project was supported in part by appointments to the Research Participation Program at the Centers for Disease Control and Prevention administered by the Oak Ridge Institute for Science and Education through an interagency agreement between the U.S. Department of Energy and the Centers for Disease Control and Prevention. We thank DVBD staff members Jason Velez for cell culture support and Sean Masters for his excellent contributions to animal husbandry and animal care needs throughout this study. The findings and conclusions of this report are those of the authors and do not necessarily represent the official position of the Centers for Disease Control and Prevention or the U.S. Agency for International Development.

## Appendix A. Supplementary data

Supplementary data to this article can be found online at https://

doi.org/10.1016/j.virol.2019.06.010.

## References


Barbosa, C.M., Di Paola, N., Cunha, M.P., Rodrigues-Jesus, M.J., Araujo, D.B., Silveira, V.B., et al., 2018. Yellow fever virus RNA in urine and semen of convalescent patient, Brazil. Epub 2017/10/24. Emerg. Infect. Dis. 24 (1). https://doi.org/10.3201/eid2401.171310. PubMed PMID: 29058663; PubMed Central PMCID: PMCPMC5749440.

Bayer, A., Lennemann, N.J., Ouyang, Y., Bramley, J.C., Morosky, S., Marques Jr., E.T., et al., 2016. Type III interferons produced by human placental trophoblasts confer protection against Zika virus infection. Epub 2016/04/14. Cell Host Microbe 19 (5), 705–712. https://doi.org/10.1016/j.chom.2016.03.008. PubMed PMID: 27066743; PubMed Central PMCID: PMCPMC4866896.

Caine, E.A., Scheaffer, S.M., Arora, N., Zaitsev, K., Artyomov, M.N., Coyne, C.B., et al., 2019. Interferon lambda protects the female reproductive tract against Zika virus infection. Epub 2019/01/19. Nat. Commun. 10 (1), 280. https://doi.org/10.1038/s41467-018-07993-2. PubMed PMID: 30655513; PubMed Central PMCID: PMCPMC6336786.

Chan, J.F., Zhang, A.J., Chan, C.C., Yip, C.C., Mak, W.W., Zhu, H., et al., 2016. Zika virus infection in dexamethasone-immunosuppressed mice demonstrating disseminated infection with multi-organ involvement including orchitis effectively treated by recombinant type I interferons. Epub 2016/11/26. EBioMedicine 14, 112–122. https://doi.org/10.1016/j.ebiom.2016.11.017. PubMed PMID: 27884655; PubMed Central PMCID: PMCPMC5161441.

Chen, J., Liang, Y., Yi, P., Xu, L., Hawkins, H.K., Rossi, S.L., et al., 2017. Outcomes of congenital Zika disease depend on timing of infection and maternal-fetal interferon action. Epub 2017/11/09. Cell Rep. 21 (6), 1588–1599. https://doi.org/10.1016/j.celrep.2017.10.059. PubMed PMID: 29117563; PubMed Central PMCID: PMCPMC5726784.

Clancy, C.S., Van Wettere, A.J., Morrey, J.D., Julander, J.G., 2018a. Coitus-free sexual transmission of Zika virus in a mouse model. Epub 2018/10/20. Sci. Rep. 8 (1), 15379. https://doi.org/10.1038/s41598-018-33528-2. PubMed PMID: 30337585; PubMed Central PMCID: PMCPMC6194026.

Clancy, C.S., Van Wettere, A.J., Siddharthan, V., Morrey, J.D., Julander, J.G., 2018b. Comparative histopathologic lesions of the male reproductive tract during acute infection of Zika virus in AG129 and ifnar(-/-) mice. Epub 2018/01/30. Am. J. Pathol. 188 (4), 904–915. https://doi.org/10.1016/j.ajpath.2017.12.019. PubMed PMID: 29378173; PubMed Central PMCID: PMCPMC5955007.

Corry, J., Arora, N., Good, C.A., Sadovsky, Y., Coyne, C.B., 2017. Organotypic models of type III interferon-mediated protection from Zika virus infections at the maternal-fetal interface. Epub 2017/08/09. Proc. Natl. Acad. Sci. U.S.A. 114 (35), 9433–9438. https://doi.org/10.1073/pnas.1707513114. PubMed PMID: 28784796; PubMed Central PMCID: PMCPMC5584447.

Diagne, M.M., Faye, M., Faye, O., Sow, A., Balique, F., Sembene, M., et al., 2017. Epub 2017/06/16. Emergence of Wesselsbron Virus Among Black Rat and Humans in Eastern Senegal in 2013, vol. 3. One health, Amsterdam, Netherlands), pp. 23–28. https://doi.org/10.1016/j.onehlt.2017.02.001. PubMed PMID: 28616499; PubMed Central PMCID: PMCPMC5454166.

Duggal, N.K., Ritter, J.M., Pestorius, S.E., Zaki, S.R., Davis, B.S., Chang, G.J., et al., 2017a. Frequent Zika virus sexual transmission and prolonged viral RNA shedding in an immunodeficient mouse model. Epub 2017/02/16. Cell Rep. 18 (7), 1751–1760. https://doi.org/10.1016/j.celrep.2017.01.056. PubMed PMID: 28199846.

Duggal, N.K., Ritter, J.M., McDonald, E.M., Romo, H., Guirakhoo, F., Davis, B.S., et al., 2017b. Differential neurovirulence of African and Asian genotype Zika virus isolates in outbred immunocompetent mice. Epub 2017/08/19. Am. J. Trop. Med. Hyg. 97 (5), 1410–1417. https://doi.org/10.4269/ajtmh.17-0263. PubMed PMID: 28820694; PubMed Central PMCID: PMCPMC5817768.

Duggal, N.K., McDonald, E.M., Ritter, J.M., Brault, A.C., 2018. Sexual transmission of Zika virus enhances in utero transmission in a mouse model. Epub 2018/03/16. Sci. Rep. 8 (1), 4510. https://doi.org/10.1038/s41598-018-22840-6. PubMed PMID: 29540804; PubMed Central PMCID: PMCPMC5852059.

Duggal, N.K., McDonald, E.M., Weger-Lucarelli, J., Hawks, S.A., Ritter, J.M., Romo, H., et al., 2019. Mutations present in a low-passage Zika virus isolate result in attenuated pathogenesis in mice. Epub 2019/02/15. Virology 530, 19–26. https://doi.org/10.1016/j.virol.2019.02.004. PubMed PMID: 30763872.

Foy, B.D., Kobylinski, K.C., Chilson Foy, J.L., Blitvich, B.J., Travassos da Rosa, A., Haddow, A.D., et al., 2011. Probable non-vector-borne transmission of Zika virus, Colorado, USA. Epub 2011/05/03. Emerg. Infect. Dis. 17 (5), 880–882. https://doi.org/10.3201/eid1705.101939. PubMed PMID: 21529401; PubMed Central PMCID: PMCPMC3321795.

Garcia-Bujalance, S., Gutierrez-Arroyo, A., De la Calle, F., Diaz-Menendez, M., Arribas, J.R., Garcia-Rodriguez, J., et al., 2017. Persistence and infectivity of Zika virus in semen after returning from endemic areas: report of 5 cases. Epub 2017/10/21. 96. the official publication of the Pan American Society for Clinical Virology, pp. 110–115. https://doi.org/10.1016/j.jcv.2017.10.006. PubMed PMID: 29053990 J. Clin. Virol.

Garcia-Nafria, J., Watson, J.F., Greger, I.H., 2016. IVA cloning: a single-tube universal cloning system exploiting bacterial in Vivo Assembly. Epub 2016/06/07. Sci. Rep. 6, 27459. https://doi.org/10.1038/srep27459. PubMed PMID: 27264908; PubMed Central PMCID: PMCPMC4893743.

Govero, J., Esakky, P., Scheaffer, S.M., Fernandez, E., Drury, A., Platt, D.J., et al., 2016. Zika virus infection damages the testes in mice. Epub 2016/11/01. Nature 540 (7633), 438–442. https://doi.org/10.1038/nature20556. PubMed PMID: 27798603; PubMed Central PMCID: PMCPMC5432198.

Huits, R., De Smet, B., Arien, K.K., Van Esbroeck, M., Bottieau, E., Cnops, L., 2017. Zika virus in semen: a prospective cohort study of symptomatic travellers returning to Belgium. Epub 2017/12/05. Bull. World Health Organ. 95 (12), 802–809. https://doi.org/10.2471/blt.17.181370. PubMed PMID: 29200521; PubMed Central PMCID: PMCPMC5710082.

Jagger, B.W., Miner, J.J., Cao, B., Arora, N., Smith, A.M., Kovacs, A., et al., 2017. Gestational stage and IFN-lambda signaling regulate ZIKV infection in utero. e3. Epub 2017/09/15. Cell Host Microbe 22 (3), 366–376. https://doi.org/10.1016/j.chom.2017.08.012. PubMed PMID: 28910635; PubMed Central PMCID: PMCPMC5647680.

Joguet, G., Mansuy, J.M., Matusali, G., Hamdi, S., Walschaerts, M., Pavili, L., et al., 2017. Effect of acute Zika virus infection on sperm and virus clearance in body fluids: a prospective observational study. Epub 2017/08/26. Lancet Infect. Dis. 17 (11), 1200–1208. https://doi.org/10.1016/s1473-3099(17)30444-9. PubMed PMID: 28838639.

Koide, F., Goebel, S., Snyder, B., Walters, K.B., Gast, A., Hagelin, K., et al., 2016. Development of a Zika virus infection model in cynomolgus macaques. Epub 2017/01/10. Front. Microbiol. 7, 2028. https://doi.org/10.3389/fmicb.2016.02028. PubMed PMID: 28066354; PubMed Central PMCID: PMCPMC5165249.

Lanciotti, R.S., Kosoy, O.L., Laven, J.J., Velez, J.O., Lambert, A.J., Johnson, A.J., et al., 2007. Genetic and serologic properties of Zika virus associated with an epidemic, Yap State, Micronesia. Epub 2008/08/06. Emerg. Infect. Dis. 14 (8), 1232–1239. https://doi.org/10.3201/eid1408.080287. PubMed PMID: 18680646; PubMed Central PMCID: PMCPMC2600394.

Lazear, H.M., Govero, J., Smith, A.M., Platt, D.J., Fernandez, E., Miner, J.J., et al., 2016. A mouse model of Zika virus pathogenesis. Epub 2016/04/14. Cell Host Microbe 19 (5), 720–730. https://doi.org/10.1016/j.chom.2016.03.010. PubMed PMID: 27066744; PubMed Central PMCID: PMCPMC4866885.

Ma, W., Li, S., Ma, S., Jia, L., Zhang, F., Zhang, Y., et al., 2016. Zika virus causes testis damage and leads to male infertility in mice. e10. Epub 2016/11/26. Cell 167 (6), 1511–1524. https://doi.org/10.1016/j.cell.2016.11.016. PubMed PMID: 27884405.

McDonald, E.M., Duggal, N.K., Brault, A.C., 2017. Pathogenesis and sexual transmission of Spondweni and Zika viruses. Epub 2017/10/07. PLoS Neglected Trop. Dis. 11 (10), e0005990. https://doi.org/10.1371/journal.pntd.0005990. PubMed PMID: 28985234.

McDonald, E.M., Duggal, N.K., Ritter, J.M., Brault, A.C., 2018. Infection of epididymal epithelial cells and leukocytes drives seminal shedding of Zika virus in a mouse model. Epub 2018/08/03. PLoS Neglected Trop. Dis. 12 (8), e0006691. https://doi.org/10.1371/journal.pntd.0006691. PubMed PMID: 30070988; PubMed Central PMCID: PMCPMC6091970.

Mead, P.S., Hills, S.L., Brooks, J.T., 2018a. Zika virus as a sexually transmitted pathogen. Epub 2017/11/28. Curr. Opin. Infect. Dis. 31 (1), 39–44. https://doi.org/10.1097/qco.0000000000000414. PubMed PMID: 29176348.

Mead, P.S., Duggal, N.K., Hook, S.A., Delorey, M., Fischer, M., Olzenak McGuire, D., et al., 2018b. Zika virus shedding in semen of symptomatic infected men. N. Engl. J. Med. 378 (15), 1377–1385. https://doi.org/10.1056/NEJMoa1711038. PubMed PMID: 29641964.

Medina, F.A., Torres, G., Acevedo, J., Fonseca, S., Casiano, L., De Leon-Rodriguez, C.M., et al., 2019. Duration of the presence of infectious Zika virus in semen and serum. Epub 2018/07/31. J. Infect. Dis. 219 (1), 31–40. https://doi.org/10.1093/infdis/jiy462. PubMed PMID: 30059980.

Moreira, J., Peixoto, T.M., Siqueira, A.M., Lamas, C.C., 2017. Sexually acquired Zika virus: a systematic review. Epub 2017/01/08. Clin. Microbiol. Infect. 23 (5), 296–305. https://doi.org/10.1016/j.cmi.2016.12.027. PubMed PMID: 28062314.

Musso, D., Roche, C., Robin, E., Nhan, T., Teissier, A., Cao-Lormeau, V.M., 2015. Potential sexual transmission of Zika virus. Epub 2015/01/28. Emerg. Infect. Dis. 21 (2), 359–361. https://doi.org/10.3201/eid2102.141363. PubMed PMID: 25625872; PubMed Central PMCID: PMCPMC4313657.

Osuna, C.E., Lim, S.Y., Deleage, C., Griffin, B.D., Stein, D., Schroeder, L.T., et al., 2016. Zika viral dynamics and shedding in rhesus and cynomolgus macaques. Epub 2016/11/01. Nat. Med. 22 (12), 1448–1455. https://doi.org/10.1038/nm.4206. PubMed PMID: 27694931; PubMed Central PMCID: PMCPMC5293594.

Palladino, M.A., Johnson, T.A., Gupta, R., Chapman, J.L., Ojha, P., 2007. Members of the Toll-like receptor family of innate immunity pattern-recognition receptors are abundant in the male rat reproductive tract. Epub 2007/02/23. Biol. Reprod. 76 (6), 958–964. https://doi.org/10.1095/biolreprod.106.059410. PubMed PMID: 17314314.

Paz-Bailey, G., Rosenberg, E.S., Doyle, K., Munoz-Jordan, J., Santiago, G.A., Klein, L., et al., 2018. Persistence of Zika virus in body fluids - final report. Epub 2017/02/15. N. Engl. J. Med. 379 (13), 1234–1243. https://doi.org/10.1056/NEJMoa1613108. PubMed PMID: 28195756; PubMed Central PMCID: PMCPMC5831142.

Sheehan, K.C., Lai, K.S., Dunn, G.P., Bruce, A.T., Diamond, M.S., Heutel, J.D., et al., 2006. Blocking monoclonal antibodies specific for mouse IFN-alpha/beta receptor subunit 1 (IFNAR-1) from mice immunized by in vivo hydrodynamic transfection. Epub 2006/11/23. J. Interferon Cytokine Res. 26 (11), 804–819. https://doi.org/10.1089/jir.2006.26.804. PubMed PMID: 17115899.

Smith, D.R., Hollidge, B., Daye, S., Zeng, X., Blancett, C., Kuszpit, K., et al., 2017. Neuropathogenesis of Zika virus in a highly susceptible immunocompetent mouse model after antibody blockade of type I interferon. Epub 2017/01/10. PLoS Neglected Trop. Dis. 11 (1), e0005296. https://doi.org/10.1371/journal.pntd.0005296. PubMed PMID: 28068342; PubMed Central PMCID: PMCPMC5249252.

Sommereyns, C., Paul, S., Staeheli, P., Michiels, T., 2008. IFN-lambda (IFN-lambda) is expressed in a tissue-dependent fashion and primarily acts on epithelial cells in vivo. Epub 2008/03/29. PLoS Pathog. 4 (3), e1000017. https://doi.org/10.1371/journal.ppat.1000017. PubMed PMID: 18369468; PubMed Central PMCID: PMCPMC2265414.

Weger-Lucarelli, J., Duggal, N.K., Bullard-Feibelman, K., Veselinovic, M., Romo, H., Nguyen, C., et al., 2017. Development and characterization of recombinant virus generated from a new world Zika virus infectious clone. Epub 2016/11/01. J. Virol. 91 (1). https://doi.org/10.1128/jvi.01765-16. PubMed PMID: 27795432; PubMed Central PMCID: PMCPMC5165210.

Zanoni, I., Granucci, F., Broggi, A., 2017. Interferon (IFN)-lambda takes the helm: immunomodulatory roles of type III IFNs. Epub 2017/12/14. Front. Immunol. 8, 1661. https://doi.org/10.3389/fimmu.2017.01661. PubMed PMID: 29234323; PubMed Central PMCID: PMCPMC5712353.

Zhu, W., Zhao, S., Liu, Z., Cheng, L., Wang, Q., Yan, K., et al., 1950. Pattern recognition receptor-initiated innate antiviral responses in mouse epididymal epithelial cells. Baltimore, Md. J. Immunol. 194 (10), 4825–4835. https://doi.org/10.4049/jimmunol.1402706. Epub 2015/04/05 PubMed PMID: 25840915.